J. Chem. Soc., Faraday Trans. 2, 1983, **79**, 1181–1194

Reduced Forms of $LaNiO_3$ Perovskite

Part 1.—Evidence for New Phases: $La_2Ni_2O_5$ and $LaNiO_2$

BY MICHEL CRESPIN, PIERRE LEVITZ AND LUCIEN GATINEAU*

Centre National de la Recherche Scientifique, Centre de Recherche sur les Solides à Organisation Cristalline Imparfaite, 1B rue de la Férollerie, 45045 Orléans, France† and L.U.R.E., Centre National de la Recherche Scientifique, Université Paris-Sud, Batiment 209, 91405 Orsay, France

Received 18*th November*, 1982

Low-temperature reduction of $LaNiO_3$ under hydrogen leads to new compounds such as $La_2Ni_2O_5$ and $LaNiO_2$ before total reduction. Hydrogen consumption, X-ray diffraction and XANES demonstrate the presence of these new phases. Ni^{3+} in $LaNiO_3$ becomes Ni^{2+} in $La_2Ni_2O_5$, and a pure monovalent nickel phase is obtained in $LaNiO_2$. After this stage nickel leaves the structure as nickel metal. Before total reduction, reversible reoxidation of $La_2Ni_2O_5$ and $LaNiO_2$ leads to the original structure of the $LaNiO_3$ perovskite.

Perovskite catalysts are widely used for the oxidation[1] of CO. $LaNiO_3$ in particular is a good candidate for use as a fuel-cell electrode.[2] In this respect their stability during heat treatment in a reducing atmosphere is one of their major advantages.

Recently, Nakamura *et al.*[3] studied the stability of $LaBO_3$-type perovskites under reducing conditions (B = V, Cr, Mn, Fe, Co, Ni). From $LaNiO_3$, at 1273 K, they obtained a mixture of La_2NiO_4 and NiO for oxygen partial pressures in the range $10^{-2} > p(O_2)/\text{Torr} > 10^{-9}$, a mixture of La_2NiO_4 and Ni^0 in the range $10^{-9} > p(O_2)/\text{Torr} > 10^{-10}$ and a total decomposition into La_2O_3 and Ni^0 for $p(O_2)/\text{Torr} < 10^{-10}$

Working at much lower temperature, between 470 and 700 K, and recirculating hydrogen we have found evidence for the existence of new phases. These have been characterized by three methods: (i) the stoichiometry is obtained from the consumption of hydrogen during the reaction; (ii) X-ray diffraction is used to insure that the new products are pure phases; (iii) the determination of the *K* adsorption edge permits an absolute determination of the nickel oxidation states in these new phases.

EXPERIMENTAL

SYNTHESIS OF $LaNiO_3$

$LaNiO_3$ was synthesized from an equimolar solution of $La(NO_3)_3 \cdot 6H_2O$ and $Ni(NO_3)_2 \cdot 6H_2O$ in water. The hydroxides were coprecipitated by adding an excess of a strong base (tetraethylammonium hydroxide). This precipitate was washed and freeze-dried. It was then calcined under flowing oxygen at 1220 K for 15 h. The X-ray diffraction patterns of the resulting product showed exclusively $LaNiO_3$ peaks. No peaks corresponding to lanthanum or nickel oxide were detected.

† Permanent address.

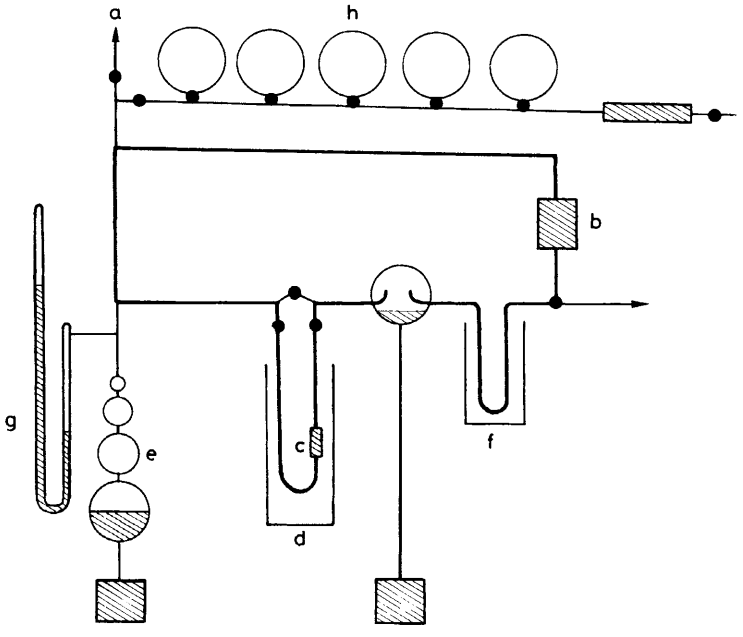

Fig. 1. Reduction apparatus: a circulation loop is connected to a conventional vacuum system (*a*). The loop is equipped with a circulation pump (*b*), a reactor (*c*) containing the sample and enclosed in a furnace (*d*), a gas burette (*e*) and liquid nitrogen as getter (*f*). A mercury manometer (*g*) is attached to the loop. Flasks (*h*) are used for storing gases (H_2, O_2 and He).

CHEMICAL IDENTIFICATION OF THE DEGREE OF REDUCTION

As shown in fig. 1, the sample was introduced into a recirculating loop which could be filled with different gases (H_2, O_2, N_2, He). Gaseous reaction products were trapped at liquid-nitrogen temperature. The sample was kept at the required temperature by means of a furnace with a precision of ±1 K. The loop was equipped with a B.E.T. system and a manometer.

After the introduction of a known quantity of $LaNiO_3$ (500 mg) the surface of the sample was cleaned by flowing oxygen at 670 K for 15 h. The apparatus was then filled with helium in order to measure the volume of the loop at the operating temperature. A known volume of hydrogen was introduced afterwards and the degree of reduction of the sample was followed by measuring the hydrogen consumption. The hydrogen consumption is measured manometrically at constant volume. The values found by this method are checked after the experiment by measuring the volume of water in the liquid-nitrogen getter.

In the domain of the temperatures investigated (<770 K) and under the conditions described above it was not possible to define the partial pressure of oxygen at the sample level and to undertake thermodynamic calculations.

X-RAY DIFFRACTION

In order to avoid reoxidation after reduction, the samples were treated in a glove box under a nitrogen atmosphere. They were examined afterwards in an vacuum chamber, using filtered Cu K_α radiation and a KCl internal standard.

EXAFS ABSORPTION EDGES

The samples were prepared in a glove box under a nitrogen atmosphere. The sample weight per cm^2 in the experimental chamber was calculated in order to obtain the maximum discontinuity of the K-edge level of nickel.[4] An adequate amount of product was suspended in a mixture of polystyrene and xylene and sedimented in a small rectangular container with a mylar base. This cell was then sealed under nitrogen pressure by a second sheet of mylar. These experiments were carried out at L.U.R.E. using synchrotron radiation from the DCI ring. The experimental device has been described earlier by Raoux *et al.*[5] Energy selection was made by a channel-cut monochromator using the 220 reflexion of silicon. The energy increments were 0.25 eV for the measurement of the absorption edge and 1.5 eV for the EXAFS spectrum. The position of the absorption edges can be defined with an accuracy of ±0.25 eV with respect to the maximum K edge of metallic copper (8991 eV).

Immediately after the measurement of the nickel absorption edge of each sample, the absorption edge of the metallic nickel was redetermined in order to avoid time-related shifts in the energy calibration.

The EXAFS spectra of nickel were recorded between 8000 and 9500 eV (the K edge of nickel is *ca.* 8335 eV). The EXAFS modulation, $\chi(E)$, is deduced from the overall absorption $\mu(E) = \ln I_0/I$ by elimination of the background signal and the normalization of the oscillations. An appropriate choice for the zero kinetic energy of the photoelectron permits one to proceed in momentum space. A Fourier transform of the $\chi(K)$ function yields the pseudo-radial distribution of the various different atoms around the nickel atom.

RESULTS AND DISCUSSION

SYNTHESIS OF REDUCED PHASES

The reduction of the samples was carried out in two different ways, either using a linearly programmed temperature mode or at a fixed temperature and various time intervals.

In the first experiment the temperature was programmed at the rate of 5 K h^{-1}. As shown in fig. 2, the hydrogen consumption (as electrons per initial $LaNiO_3$ molecule) is plotted against temperature. The slope of the curve undergoes abrupt changes at three points corresponding exactly to 1, 2 and 3 electrons per $LaNiO_3$ molecule. The overall reaction scheme can be written as follows:

$$LaNiO_3 + xH_2 \rightarrow LaNiO_{3-x} + xH_2O. \quad (1)$$

Isothermal reductions were carried out at 550, 590, 670 and 770 K, as shown in fig. 3. The discontinuity at 1 electron per $LaNiO_3$ in the reaction kinetics appears throughout this temperature domain. The discontinuities at the 2 and 3 electron levels appear at 590 K or at 670 and 770 K, respectively.

Samples were examined by X-ray diffraction at different degrees of reduction. Using the overall stoichiometry as described by reaction (1) the following phases were characterized: $LaNiO_3$, $LaNiO_{2.5}$, $LaNiO_2$, $LaNiO_{1.5}$, and intermediate phases between $LaNiO_3$ and $LaNiO_{2.5}$. The chemical composition of the samples is determined within a maximum deviation of 0.02 in the oxygen content.

X-RAY DIFFRACTION

$LaNiO_3$

A rhombohedral pseudo unit cell was proposed by Wold *et al.*[6] for $LaNiO_3$ with the following parameters: $a = 7.676 \pm 0.002$ Å and $\alpha = 90.72°$, together with a primitive rhombohedral cell with $a = 5.641$ Å and $\alpha = 60.82°$ (the corresponding

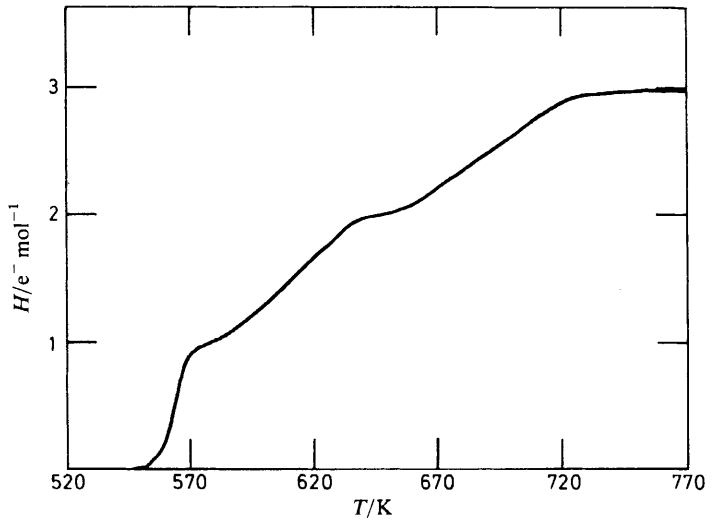

Fig. 2. Plot of hydrogen consumption, H (electron per mol $LaNiO_3$), as a function of temperature, T, at a constant rate of temperature increase (5 K h^{-1}).

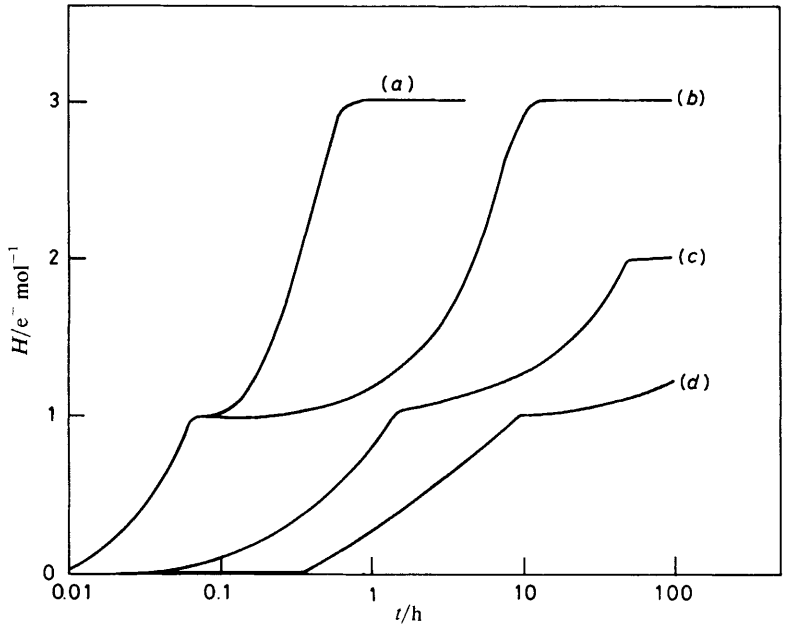

Fig. 3. Plot of hydrogen consumption, H (electron per mol $LaNiO_3$), as a function of time, t, at different temperatures: (*a*) 770, (*b*) 670, (*c*) 585 and (*d*) 550 K.

Table 1. X-ray powder data for $LaNiO_3$ described in the rhombohedral and hexagonal systems

hkl (rhombohedral)	d_{obs}	d_{calc}	I	*hkl* (hexagonal)
110	3.839	3.837	25	012
$\bar{1}10$	2.730	2.729	100	110
211	2.698	2.697	85	104
200	2.224	2.224	25	202
222	2.189	2.190	10	006
220	1.918_7	1.918_3	60	024
$21\bar{1}$	1.723_9	1.723_8	10	122
321	1.708_1	1.707_8	10	116
$\bar{2}11$	1.575_0	1.575_5	20	300
310	1.569_4	1.569_3	40	214
332	1.551_1	1.551_2	15	018
$\bar{2}20$	1.364_5	1.364_4	15	220
422	1.348_6	1.348_6	15	208
$\bar{3}10$	—	1.285_5	<5	312
411–330	1.279_1	1.278_8	5	306
433	—	1.265_8	<5	1010
$32\bar{1}$	1.217_3	1.217_5	10	134
431	1.208_9	1.209_0	10	128
$\bar{2}22$	—	1.163_0	<5	402
420	1.157_8	1.158_0	5	226
442	—	1.148_3	<5	0210

hexagonal cell has $a = 5.456$ Å, $c = 13.122$ Å). We have redetermined these parameters on our starting material using KCl as an internal standard. The diffraction data found for this sample are given in table 1. The following values are found for the cell parameters of the pseudo-cell: $a = 7.674 \pm 0.002$ Å and $\alpha = 90.66 \pm 0.01°$. The primitive rhombohedral cell that can be deduced from these has the following parameters: $a = 5.395$ Å, $\alpha = 60.77°$ (the hexagonal cell has $a = 5.458$ Å, $c = 13.138$ Å). The differences found between the parameters of the rhombohedral cell as published by Wold *et al.* and those determined in our laboratory are due to a mathematical error when using of the rhombohedral–hexagonal transformation formulae in Wold's calculations. The indices given in table 1 refer to the rhombohedral cell ($a = 5.395$ Å, $\alpha = 60.77°$) and the corresponding hexagonal cell. The indices published by Wold *et al.* refer to a rhombohedral cell with $a = 3.838$ Å, $\alpha = 90.72°$.

$LaNiO_{2.5}$

At this stage of the reduction, the stoichiometry obtained volumetrically can follow from either

$$2LaNiO_3 + H_2 \rightarrow La_2NiO_4 + NiO + H_2O \quad (2)$$

or

$$2LaNiO_3 + H_2 \rightarrow La_2Ni_2O_5 + H_2O. \quad (3)$$

La_2NiO_4 has been identified by Rabenau and Eckerlin.[7] Nakamura *et al.*[3] obtained a mixture of La_2NiO_4 and NiO after reduction of $LaNiO_3$ at 1273 K. The product

Table 2. X-ray powder data for $La_2Ni_2O_5$

hkl	d_{obs}	d_{calc}	*I*
002	3.908	3.909	30
$10\bar{2}$	3.734	2.731	10
040	2.791	2.792	30
400	2.764	2.765	100
$03\underline{2}$	2.698	2.696	50
$40\bar{1}$	2.640	2.639	10
330	2.618	2.620	20
042	2.272	2.272	10
$40\underline{2}$	2.216	2.217	5
$30\bar{3}$	2.168	2.168	10
004	1.952	1.955	35
$20\bar{4}$	1.864	1.866	10
620	1.745	1.750	10
$45\underline{1}$	1.685	1.688	<5
$62\bar{2}$	1.618	1.620	10
262	1.596	1.601	5
144	1.581	1.578	10
$42\bar{4}$	1.561	1.561	5
443	1.549	1.549	5
424	1.511	1.509	<5
800	1.381	1.383	5

Table 3. Comparison of $LaNiO_3$ parameters derived for a monoclinic lattice with $La_2Ni_2O_5$ and $LaNiO_{2.7}$ parameters

stoichiometry	*a*/Å	*b*/Å	*c*/Å	*α*/°	*β*/°	*γ*/°	V/Å^3
$LaNiO_3$	10.790	10.915	7.674		90.94		904
$La_2Ni_2O_5$	11.068	11.168	7.824		92.21		966
$La_2Ni_2O_5/LaNiO_3$	1.026	1.023	1.020				
$LaNiO_{2.7}$	10.831	10.906	7.813	90.80	93.67	90.82	920
$LaNiO_{2.7}/LaNiO_3$	1.004	0.999	1.018				

we obtained by reduction at low temperatures has a diffraction diagram completely different from La_2NiO_4 and shows no NiO diffraction lines. However, it can be indexed as a monoclinic phase with the following parameters: $a = 11.068 \pm 0.002$ Å, $b = 11.168 \pm 0.002$ Å, $c = 7.824 \pm 0.002$ Å, $\beta = 92.21 \pm 0.01$ °.

A comparison between the observed distances and the distances calculated from the proposed unit cell is given in table 2. It demonstrates the evidence for the existence of a single phase with the stoichiometry $La_2Ni_2O_5$.

We can also compare (table 3) the previously mentioned parameters with the $LaNiO_3$ parameters for a monoclinic cell, with as edges *a* and *b* the diagonals of one face of the pseudo-cell (with 8 units per cell) and as *c*, the edge of this pseudo-cell (fig. 4). By this it can be shown that practically identical growth is observed on the *a*, *b* and *c* parameters. Consequently the monoclinic cell of $La_2Ni_2O_5$ might contain as many as 8 patterns per unit cell.

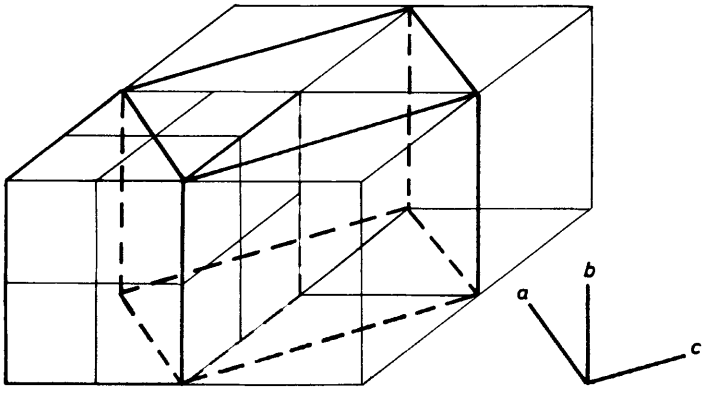

Fig. 4. Monoclinic representation of the $LaNiO_3$ unit cell.

$LaNiO_2$

At this stage of the reduction the overall reaction equation mentioned above can be written in three ways:

$$2LaNiO_3 + 2H_2 \rightarrow La_2NiO_4 + Ni + 2H_2O \quad (4)$$

$$4LaNiO_3 + 4H_2 \rightarrow La_2Ni_2O_5 + 2Ni + La_2O_3 + 4H_2O \quad (5)$$

or

$$LaNiO_3 + H_2 \rightarrow LaNiO_2 + H_2O. \quad (6)$$

Nakamura *et al.*[3] have published evidence of the products of reaction (4) under reduction at 1273 K.

Under our reduction conditions above 670 K, we found a mixture of $La_2Ni_2O_5$ and La_2O_3, which seems to correspond to reaction (5). Metallic nickel is not observed by X-ray diffraction, which must imply that it is present in the form of very small crystallites, as will be explained below.

However, when the reaction is carried out below 670 K, a single phase is formed which can be indexed in the tetragonal system with the following parameters: $a = b = 3.966 \pm 0.001$ Å, $c = 3.376 \pm 0.001$ Å. A comparison between the observed distances and those calculated from this unit cell is given in table 4.

The single phase corresponds to reaction (6). In the $LaNiO_2$ phase nickel must exist in the oxidation state +1. The oxidation state of monovalent nickel has scarcely been observed. The existence of Ni^+ will be confirmed by the position of K absorption edge in a later article. The $LaNiO_2$ structure will be described in further detail using an X-ray powder diagram and EXAFS spectroscopy of nickel.

$LaNiO_{1.5}$

At this stage of the reduction the reaction can be written as follows:

$$2LaNiO_3 + 3H_2 \rightarrow La_2O_3 + 2Ni + 3H_2O. \quad (7)$$

When this reaction is carried out at 670 K La_2O_3 is the only phase which has been observed by X-ray diffraction.

Table 4. X-ray powder data for $LaNiO_2$

hkl	d_{obs}	d_{calc}	*I*
010	3.968	3.966	35
001	3.376	3.376	<5
110	2.804	2.804	75
011	2.570	2.571	100
111	2.157	2.157	20
200	1.983	1.983	45
120	1.773	1.774	5
021	1.708	1.710	<5
002	1.685	1.688	5
121	1.569	1.570	35
012	—	1.553	<5
112	1.444	1.446	5
220	1.401	1.402	10
030	—	1.322	<5
221	—	1.295	<5
022	1.285	1.285	5
130	1.252	1.254	5
031	1.229	1.231	5
122	—	1.223	<5
131	1.175	1.176	<5

Only after heating at 1070 K in an inert atmosphere do nickel peaks appear in the diagram. One may thus conclude that after reduction at 670 K nickel is present either as an amorphous phase or as very small particles undetectable by conventional X-ray diffraction (diameter <25 Å).

INTERMEDIATE PHASE

The reduction can be interrupted when in $LaNiO_{3-x}$, $x<0.5$. In this case from the beginning of reduction ($LaNiO_{2.95}$) a new phase appears which does not change until the overall stoichiometry of $LaNiO_{2.70}$ is reached. The compound that is formed can be described as a triclinic cell with the following parameters: $a = 10.831 \pm 0.002$ Å, $b = 10.906 \pm 0.002$ Å, $c = 7.813 \pm 0.002$ Å, $\alpha = 90.80 \pm 0.01$ °, $\beta = 93.67 \pm 0.01$ °, $\gamma = 90.82 \pm 0.01$ °. With respect to the monoclinic cell of $LaNiO_3$ (fig. 4), table 3 shows that only the *z*-axis is affected (by 2%). Table 5 represents the observed spacings for $LaNiO_{2.7}$ and line indices computed from the parameters mentioned above.

The spacings observed for $LaNiO_{2.9}$ and $LaNiO_{2.8}$ do not differ from those mentioned in table 5 by more than 0.005 Å. The relative intensities of the strongest reflexions, 400, 040 and 211, however, can vary from 10 to 20%.

The product corresponding to the reduction stage $LaNiO_{2.6}$ exhibits an X-ray diffraction pattern identical with that observed for $LaNiO_{2.5}$ as far as the position of the peaks is concerned. However, the relative intensities are distinctly modified, particularly for the 032 ($I = 100$), 402 ($I = 20$) and 144 ($I = 30$) reflexions.

At the stoichiometry $LaNiO_{2.68}$ we observed a superposition of the diffraction patterns of $LaNiO_{2.7}$ and $LaNiO_{2.5}$. In the course of the reduction there is a small transition domain where two phases coexist. $LaNiO_{2.68}$ is stoichiometrically very close to $La_3Ni_3O_8$; unlike Lander,[8] who found a single phase for $Ba_3Ni_3O_8$, we found a mixture of two phases.

Table 5. X-ray powder data for $LaNiO_{2.7}$

hkl	d_{obs}	d_{calc}	*I*
002	3.899	3.898	15
$2\bar{2}0$	3.869	3.868	20
220	3.813	3.809	5
$\bar{1}02$	3.747	3.744	5
231	2.753	2.752	50
040	2.726	2.726	90
400	2.702	2.702	100
$\bar{3}12$	2.653	2.653	5
042	2.222	2.218	20
004	1.949	1.949	20
$4\bar{4}0$	1.933	1.934	30
440	1.904	1.905	15
$\bar{2}04$	1.872	1.872	5
314	1.740	1.741	<5
$03\bar{4}$	1.728	1.728	5
$26\bar{1}$	1.687	1.687	<5
$(2\bar{6}2)(\bar{4}43)$	1.577	1.578	35
361	1.566	1.566	15
262	1.549	1.550	10
272	1.378	1.378	5
080	1.363	1.363	5
800	1.350	1.351	10
$\bar{6}44$	1.223	1.223	5

The nature of the mixture of intermediate compounds between $La_2Ni_2O_5$ and the completely reduced product (La_2O_3 + Ni) depends on the treatment temperature. At 590 K a mixture of $La_2Ni_2O_5$ and $LaNiO_2$ is obtained. After 100 h reduction at this temperature the reaction does not proceed beyond $LaNiO_2$ (fig. 3). For temperatures >670 K $LaNiO_2$ is not observed, and the X-ray diagram shows a mixture of $La_2Ni_2O_5$ and La_2O_3. The nickel phase itself is not seen, owing to the small dimensions of the nickel crystallites. During the reduction the $La_2Ni_2O_5$ phase diminishes progressively until it completely disappears.

X-RAY ABSORPTION SPECTROSCOPY

The position of the absorption edges of nickel at the various different stages of reduction has allowed us to determine the oxidation state of nickel and to choose between the different reaction pathways corresponding to the overall formula $LaNiO_{3-x}$.

The L_{III} absorption edge of lanthanum remained constant at 5480 eV in all the samples. This observation was predictable, because of the high electronegativity of this element. However, it was necessary to check this point in order to explain all the results without ambiguity.

K-EDGE ABSORPTION OF NICKEL

Fig. 5 shows the *K* edges of nickel in $LaNiO_3$, $La_2Ni_2O_5$, La_2NiO_4 and $LaNiO_2$ following calibration with metallic nickel. All these curves have the same general shape. A first transition of weak intensity is observed at 8330 eV which is generally attributed to a forbidden dipolar electric transition $1s \rightarrow 3d$. This is partially allowed

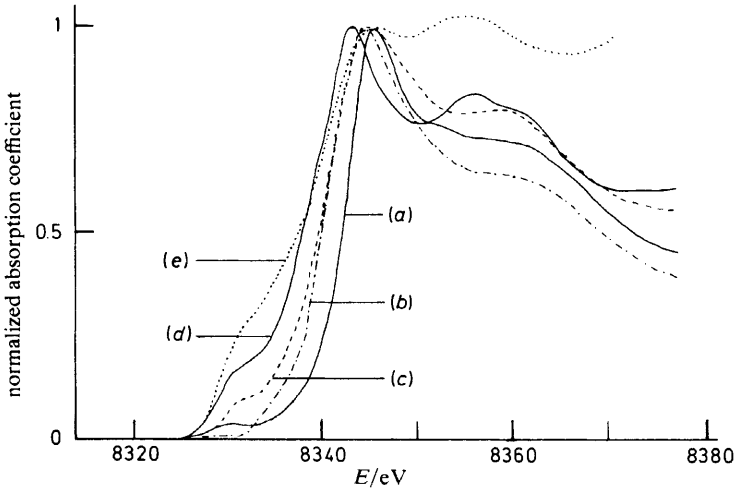

Fig. 5. Energy position, E, of the K absorption edge of nickel in (a) $LaNiO_3$, (b) La_2NiO_4, (c) $LaNiO_{2.5}$, (d) $LaNiO_2$ and (e) a sheet of nickel metal.

by an overlap between the $3d$ nickel orbitals with the $2s$ and $2p$ oxygen-ligand orbitals. This transition is followed by the major peak of the absorption edge, which is attributed to dipolar electric transitions of the $1s \rightarrow 4p$ type.[9,10] These edges are displaced as a function of the positive charge on the nickel ion. Fig. 5 shows a shift of 2 eV to lower energies between $LaNiO_3$ and $La_2Ni_2O_5$ and between $La_2Ni_2O_5$ and $LaNiO_2$.

As shown in fig. 6, a linear relationship exists between the oxidation state of nickel and the position of the principal inflexion point of the K-edge absorption spectra of the stoichiometries between $LaNiO_3$ and $LaNiO_2$. Note that it is impossible to obtain the shape of the K absorption-edge spectra of $La_2Ni_2O_5$ and $LaNiO_2$ by a linear combination of the absorption edges of metallic nickel and $LaNiO_3$. Consequently, the valence states +2 and +1 can unambiguously be attributed to nickel in $La_2Ni_2O_5$ and $LaNiO_2$, respectively. In the intermediate phases between $LaNiO_3$ and $La_2Ni_2O_5$, nickel is present as Ni^{3+} and Ni^{2+}. These compounds can be represented by the general formula $La(Ni^{3+}_{1-2x}Ni^{2+}_{2x})O_{3-x}$.

In fig. 7 the K absorption edge of nickel of the completely reduced species ($LaNiO_{1.5}$) and that determined from a sheet of metallic nickel are shown. Two identical curves are obtained, which confirms the presence of metallic nickel in this sample in spite of the absence of nickel diffraction lines in the X-ray spectrum.

EXAFS OF NICKEL IN $LaNiO_{1.5}$

The EXAFS spectrum gives information concerning the organization of metallic nickel in the final phase of reduction [reaction (7)]. Fig. 8 shows the form of the pseudo-radial distribution around the nickel atoms for the completely reduced sample and for a sheet of nickel metal. These two curves are obtained by treating the EXAFS oscillations with the same apodization condition of Fourier transform and with an identical zero for the kinetic energies of the photoelectrons. The shapes of the two radial distributions remain very similar within a distance of 10 Å. They differ only by a proportionality factor.

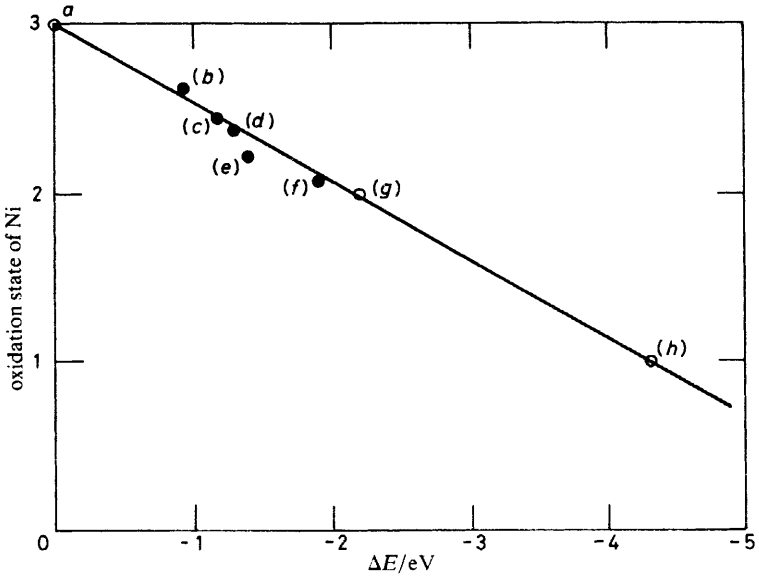

Fig. 6. Oxidation state of nickel in different phases formed during reduction of $LaNiO_3$ plotted against the energy shift of the absorption edge using $LaNiO_3$ as a standard: (*a*)$LaNiO_3$, (*b*) $LaNiO_{2.8}$, (*c*) $LaNiO_{2.7}$, (*d*) $LaNiO_{2.68}$, (*e*) $LaNiO_{2.6}$, (*f*) La_2NiO_4, (*g*) $LaNiO_{2.5}$ and (*h*) $LaNiO_2$.

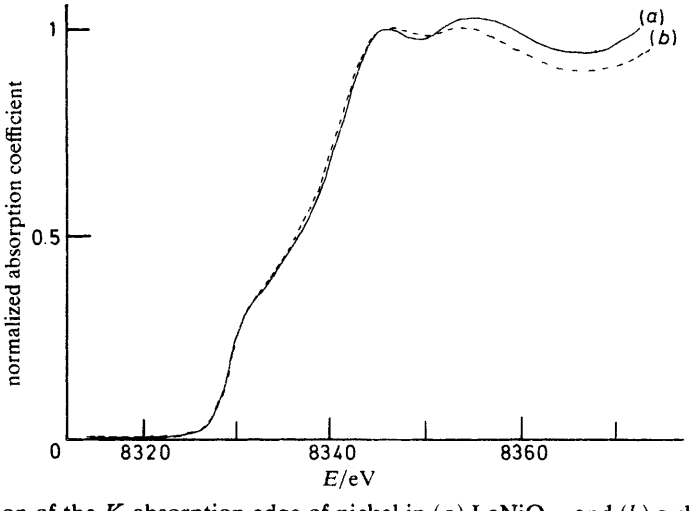

Fig. 7. Position of the *K* absorption edge of nickel in (*a*) $LaNiO_{1.5}$ and (*b*) a sheet of nickel metal.

In the final stage of reduction the overall formula $LaNiO_{1.5}$ corresponds to a mixture of La_2O_3 and metallic nickel. The nickel is present as small crystallites with the same face-centred cubic structure as in bulk nickel. The dimensions of these particles must be between 10 and 25 Å, which are the detection limits of EXAFS and X-ray diffraction, respectively.

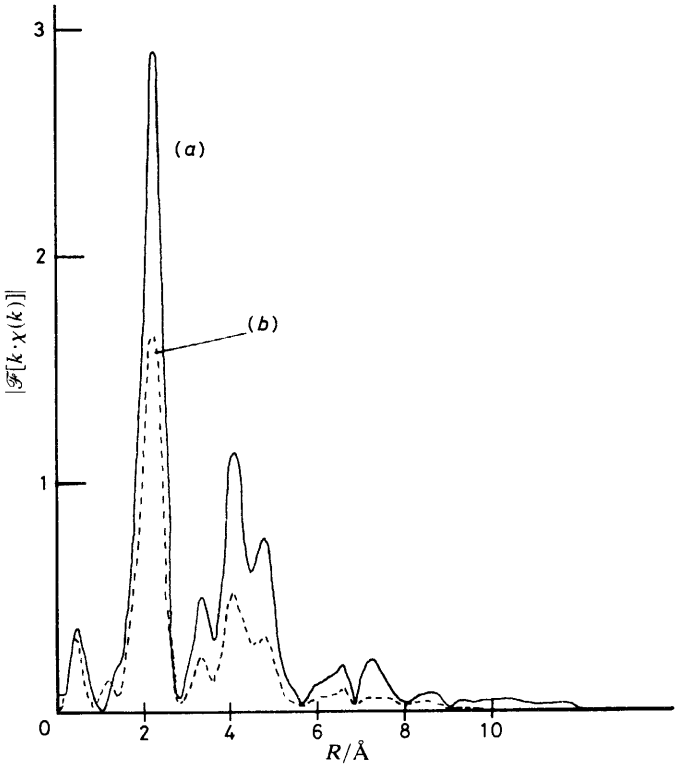

Fig. 8. Fourier-transform magnitude, $\mathcal{F}$, of K-weighted EXAFS of (*a*) a sheet of nickel metal and (*b*) $LaNiO_{1.5}$.

STABILITY OF THESE COMPOUNDS

All the compounds described above are stable in air at normal temperatures and pressures. The X-ray diffraction diagrams of all the compounds obtained after 15 days atmospheric exposure remained unchanged.

However, after heating at 1273 K in the presence of helium, the compounds $La_2Ni_2O_5$ and $LaNiO_2$ displayed X-ray diagrams corresponding to the dismutation reaction

$$La_2Ni_2O_5 \rightarrow La_2NiO_4 + NiO \quad (8)$$

$$2LaNiO_2 \rightarrow La_2NiO_4 + Ni. \quad (9)$$

It was shown earlier that in the case of the completely reduced sample heating at 1270 K resulted in recrystallization of the metallic nickel.

REOXIDATION OF THESE COMPOUNDS

Under flowing oxygen at 400 Torr and 450 K $La_2Ni_2O_5$ is reoxidized to $LaNiO_3$. This $LaNiO_3$ is well crystallized and shows a good separation of the $\bar{1}10$ and 211 doublet in the X-ray diagram. Under the same conditions of reoxidation a strongly

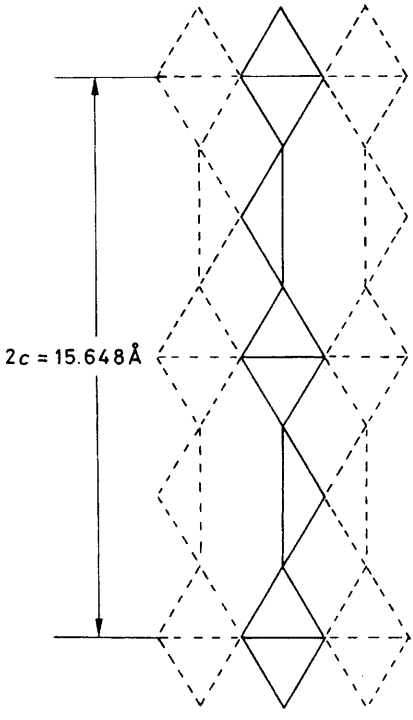

Fig. 9. Proposed structure for $La_2Ni_2O_5$: each corner is an oxygen atom. Nickel atoms are located in distorted octahedra and tetrahedra.

exothermal reaction is observed with $LaNiO_2$, resulting in overheating of the sample. The resulting $LaNiO_3$ has a smaller degree of crystallinity. For the completely reduced phase a strongly exothermal reaction is observed and the product obtained is a mixture of La_2NiO_4 and NiO.

STRUCTURE

The structure of $LaNiO_2$ being highly symmetrical, it could eventually be elucidated from the powder diagram. This result is given in the following article, where the proposed structure is confirmed by the interatomic distances around the nickel atom obtained by EXAFS.

For $La_2Ni_2O_5$, however, it is impossible to solve the structure from the twenty reflexions observed for the powder. A model can be proposed by analogy with the structure of $Ca_2Fe_2O_5$ found by Bertaut *et al.*[11] These results have been presented in an idealized form by Grenier *et al.*[12] Perpendicular to the *y* axis of this compound a succession of planes is observed, composed of octahedra and tetrahedra around the iron atoms. An identical environment can be proposed for nickel in $La_2Ni_2O_5$ (fig. 9), where a succession of planes is found parallel to the 001 plane of the monoclinic lattice. Such a representation, however, implies a doubling of the *c* parameter that we have computed or the existence of a non-centrosymmetric structure with tetrahedra lying in the same direction in two successive planes. Only a detailed study using a monocrystal can confirm this model.

CONCLUSIONS

The reaction temperature is indeed the factor determining the nature of the phases that are obtained by reducing $LaNiO_3$. $LaNiO_2$ is obtained only between 570 and 670 K, while total reduction ($La_2O_3 + Ni$) is reached only at 670 K or above. A mixture of phases, including La_2NiO_4, is only obtained at a much higher temperature[3] (1270 K).

The structural evolution in the course of the reduction is discontinuous. From $LaNiO_{2.95}$ an abrupt variation in symmetry is observed, changing from rhombohedral to triclinic. For $LaNiO_{2.68}$ the reduced product is a mixture of different phases. These results are very different from those published by Grenier *et al.*,[11] who found evidence for the evolution of the parameters in $CaTi_{1-2v}Fe_{2v}O_{3-v}$.

We think that it is now established that nickel in the $LaNiO_2$ phase is in the oxidation state +1. It is important to note that, in contrast to the few other examples of nickel in the +1 state,[13,14] $LaNiO_2$ is stable in air up to 450 K.

We are grateful for fruitful discussions and helpful assistance of Prof. J. Petiau, Prof. G. Calas and Dr H. Nijs and the team of L.U.R.E.

1 R. J. H. Voorhoeve, J. P. Remeika and L. E. Trimble, *Ann. N.Y. Acad. Sci.*, 1976, **272**, 3.
2 R. E. Martin, NASA Document, CR-159807, FCR-1657 (1980).
3 T. Nakamura, G. Petzow and L. J. Gauckler, *Mater. Res. Bull.*, 1979, **14**, 649.
4 *International Tables for X-ray Crystallography* (Kynoch Press, Birmingham, 1965), vol. 4.
5 D. Raoux, J. Petiau, P. Bondot, G. Calas, A. Fontaine, P. Lagarde, P. Levitz, G. Loupias and A. Sadoc, *Rev. Phys. Appl.*, 1980, **15**, 1079.
6 A. Wold, B. Post and E. Banks, *J. Am. Chem. Soc.*, 1957, **79**, 4911.
7 A. Rabenau and P. Eckerlin, *Acta Crystallogr.*, 1958, **11**, 304.
8 J. J. Lander, *Acta Crystallogr.*, 1951, **4**, 148.
9 J. Petiau, G. Calas, P. Bondot, C. Lapeyre, P. Levitz and G. Loupias, International Meeting at Daresbury, 1981, *EXAFS in Inorganic Systems*, ed. C. D. Garner and S. S. Hasnain (S.E.R.C., Daresbury, 1981).
10 A. Bianconi, International Meeting at Daresbury, 1981, *EXAFS in Organic Systems*, ed. C. D. Garner and S. S. Hasnain (S.E.R.C., Daresbury, 1981).
11 E. Bertaut, P. Blum and A. Sagniere, *Acta Crystallogr.*, 1959, **12**, 149.
12 J. C. Grenier, M. Pouchard, P. Hagenmuller, C. Schiffmacher and P. Caro, *J. Phys. (Paris) Colloq.*, 1977, **C7**, 84.
13 A. Gleizes, M. Dartiguenave, Y. Dartiguenave, J. Galy and H. F. Klein, *J. Am. Chem. Soc.*, 1977, **99**, 5187.
14 W. Hayes and J. Wilkens, *Proc. R. Soc. London, Ser. A*, 1964, **281**, 340.

(PAPER 2/1939)